

The flat X-ray spectrum of the LINER NGC 1052

M. Guainazzi¹, L.A. Antonelli²

¹*Astrophysics Division, Space Science Department of ESA, ESTEC, Postbus 299, NL-2200 AG Noordwijk, The Netherlands*

²*Osservatorio Astronomico di Roma, Via dell'Osservatorio 5, I-00040 Monteporzio Catone, Italy*

7 October 2018

ABSTRACT

We report on ROSAT and ASCA observations of the LINER NGC 1052, which is the first one where broad optical lines in polarized light have been observed. The 2–10 keV spectrum is very flat, with a $\Gamma_{\text{observed}} \simeq 0.1$. A model where a nuclear source is - partly or totally - obscured by a screen of matter with column density $\sim 10^{23} \text{ cm}^{-2}$ is the most convincing explanation for the observed flatness. This agrees with the hypothesis that the LINERs are a population of low-luminosity AGN, to which the Seyfert unification scenario applies. The *intrinsic* spectral index is still rather flat ($\Gamma_{\text{intrinsic}} \simeq 1.0\text{--}1.4$), as observed in a few type-2 Seyferts so far or predicted if the accretion occurs in an advection-dominated flow.

Key words: Galaxies: individual: NGC 1052 – X-rays: galaxies – accretion disks

1 INTRODUCTION

It is still a matter of debate whether Low Ionization Nuclear Emission Line Regions Galaxies (LINERs) are powered by intense starbursts, or by an active galactic nucleus (AGN), or both. In some well-studied LINERs the non-stellar nature is almost certain (*e.g.*: M81, M87, M104). However, for the majority of objects the existence or relative amount of the AGN contribution remains unknown. Several facts point in favor of the idea that most LINERs are low-luminosity AGN: the similarity in the host galaxy properties and magnitude distribution (Ho et al. 1997), the discovery of supermassive black holes in the central regions (Ho 1998), and of broad wings of permitted optical lines (Ho 1999).

Studies in the X-rays allow in principle to probe the innermost regions of the galaxies up to a few Schwarzschild radii around the putative central black hole and to investigate the high-energy processes in the surrounding environment. Actually, soft compact X-ray emission has been detected in a handful of LINERs by the ROSAT HRI (Worral & Birinkshaw 1994; Koratkar et al. 1995; Fabbiano & Juda 1997), but the instrumental spatial resolution allowed to limit the extension of the emitting region no better than about a few hundred pc. The ASCA observation of LINERs revealed that a “canonical” simple model is a general good description of the observed spectra, which is composed by a hard power-law with photon index $\Gamma \simeq 1.7\text{--}1.8$ and a soft excess of thermal origin, with typical temperatures $\simeq 1 \text{ keV}$ (see Ptak et al. 1998 and references therein). Although the latter component closely resembles the non-thermal power-law commonly observed in Seyfert 1s, the lack of iron K_{α}

line emission (Terashima et al. 1998) argues against this identification.

If the LINERs are indeed a low-luminosity and nearby population of Seyfert-like objects, one might expect that the Seyfert unification scenario (see Antonucci 1993 for a review) applies to them as well and that a population of LINERs exists, where the Broad Line Region is hidden by optically thick matter. Actually, only a fraction of the observed LINERs shows broad optical lines (Ho 1999). A substantial support to this hypothesis has come from the recent discovery of a broad H_{α} line in the polarized light spectrum of the prototypical LINER NGC 1052 (Barth 1998), confirming previous weaker claims (Ho et al. 1997).

If the above interpretation is correct, in some LINERs one might observe X-ray spectra that are analogous to the ones typically observed in Seyfert 2 galaxies: either a power-law spectrum is seen in transmission through a $N_{\text{H}} \sim 10^{21\text{--}24} \text{ cm}^{-2}$; or, if the absorbing matter is optically thick to Compton scattering ($N_{\text{H}} \gtrsim 10^{24} \text{ cm}^{-2}$), only the reflection of the nuclear radiation is detected. The last case has been observed in a handful of so-called “Compton-thick” sources (Iwasawa et al. 1997; Matt et al. 1996a, 1996b, 1997; Maiolino et al. 1998), including the LINER NGC 6240 (Iwasawa & Comastri 1998).

NGC 1052 is an elliptical galaxy ($3' \times 2'.1$) at a distance of about 28 Mpc (or $z = 0.0049$, De Vaucouleurs 1991), with $m_{\text{B}} = 11.8$. It is a LINER (Heckman 1980; Sadler 1987), located in the group HG 44 (Huchra & Geller 1982; Garcia 1993), whose barycenter lies about 8' North from NGC 1052. Optical and UV observations show an extended (20") emission line region with shock heating emission spectrum (Fosbury et al. 1978; 1981) and an IR excess, which is confined

Table 1. Observation log

Instrument	Date	Exposure time (ks)
HRI	04/08/94	$\simeq 3.4$
HRI	02/10/95	$\simeq 22$
PSPC	23/07/1993	$\simeq 14$
ASCA	12/08/1996	$\simeq 36$ (SIS)
		$\simeq 38$ (GIS)

to a central region smaller than $2''$ ($\simeq 300$ pc) and coincident with the optical nucleus. This suggests that IR emission could arise from dust heated by the non-thermal source observed in optical and UV (Becklin et al., 1982). NGC 1052 is a strong radio source and its radio spectrum peaks at the GHz frequencies. The spectrum is flatter than $\alpha = -0.9$ above 1 GHz and is variable on a timescales of months (Disney & Wall 1977). VLBI observations showed a compact radio core with a diameter of 0.001 arcsec ($\simeq 0.14$ pc) and a radio halo of about 21 arcsec (Fosbury et al. 1978). Recently very luminous water masers have been detected toward this source (Claussen et al. 1998), which are not aligned perpendicular to the radio jet, like in NGC 4258 and NGC 1068, but rather lie along the jet at a distance of 0.07 pc from the central engine. This implies that masers emission in NGC 1052 should be associated with radio jet or radio continuum rather than with a molecular region orbiting around the central engine (like in NGC 4258).

In this *Letter* we report still unpublished results on observations of NGC 1052 taken by the ROSAT and ASCA X-ray observatories. Statistical uncertainties are quoted at 90% level of confidence for one interesting parameter ($\Delta\chi^2 = 2.71$); energies are quoted in the source rest frame; $H_0 = 50 \text{ km s}^{-1} \text{ Mpc}^{-1}$ and $q_0 = 0.5$ are assumed, unless otherwise specified.

2 DATA PREPARATION

Data of NGC 1052 have been retrieved from the ASCA and ROSAT public archives as screened event file lists, which have been pre-processed and reduced according to standard criteria. The log of the observations presented in this *Letter* is reported in Table 1

The ROSAT/PSPC is a Position Sensitive Proportional Counter sensitive in the 0.1–2.0 keV band with a spatial resolution of about $20''$ for on-axis sources. Scientific products have been extracted from a circular area of $1'$, which includes 99.5% of the 0.2 keV source photons (and an even higher fraction at higher energies). The background spectrum has been extracted from an annulus with internal radius of $3'$ and external radius of $5'$ draw around the source. In the analysis of PSPC spectra we eliminated PHA channels below 9 and above 200 due to calibration uncertainties. ROSAT/HRI is a High Resolution Imager with a spatial resolution of about $10''$ and a limited (2-band) spectral response. ASCA payload (Tanaka et al. 1994; Makishima et al. 1996) is constituted by a pair of Charge Couple Devices (Solid Imaging Spectrometers, SIS0 and SIS1), sensitive in the 0.6–9 keV band, and a pair of gas scintillating proportional counters (Gas Imaging Spectrometers, GIS2 and GIS3), sensitive in the 0.7–10 keV band. Only grade 0,1,2 and 4 of the SIS data

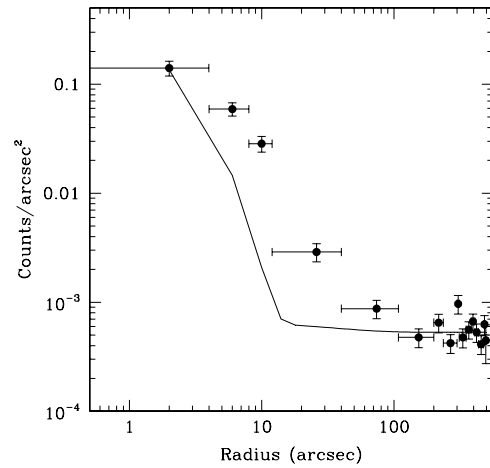


Figure 1. Radial profile of the combined NGC 1052 HRI observations (*circles*), superimposed to the instrumental PSF, as determined from the white dwarf HZ 43 profile (*solid line*). The instrumental background (field of view average count rate $5.4 \times 10^{-3} \text{ arcsec}^{-2}$) is accounted by a constant plateau in the PSF. Each data point has a signal-to-noise ratio 5

have been used. Scientific products have been extracted from circular areas of $4'$, $3.25'$ and $6'$ around the apparent centroid of the source, for the SIS0, SIS1 and GIS, respectively, including more than 99% of the source photons. To remove any possible contamination from HG 44, background spectra have been extracted using the complement area of the same chip where the source lies and from an annulus surrounding the source extraction region and having its same area for the SIS and GIS, respectively. The following results are not substantially affected if different regions of the detectors' field of views or spectra extracted from blank sky fields are employed. NGC 1052 is well above the background up to 8 and 10 keV in the SIS and the GIS, respectively. Spectra have been rebinned in order to have at least 20 counts per channel, in order to ensure the applicability of the χ^2 test. Total count rates are: 0.0519 ± 0.0014 , 0.0376 ± 0.0012 , 0.0403 ± 0.0013 , 0.0436 ± 0.0015 , and $0.0311 \pm 0.0017 \text{ s}^{-1}$ for the SIS0, SIS1, GIS2, GIS3 and PSPC, respectively.

3 SPATIAL AND TIMING ANALYSIS

In Fig. 1 the NGC 1052 radial profile extracted from the combined image of the two HRI observations is compared with the instrumental Point Spread Function (PSF). NGC 1052 shows extension up to $100''$, which is likely to be associated with the diffuse emission of the galaxy. The count rate associated with the extended component is 0.168 s^{-1} . It correspond to a 0.1–2 keV The luminosity of $\sim 3 \times 10^{40} \text{ erg s}^{-1}$, if one assumes a thermal bremsstrahlung with temperature 0.5 keV and seen through an absorbing column density of $3 \times 10^{20} \text{ cm}^{-2}$. No appreciable variability is detected, either in the ASCA 0.5–1.5 and 1.5–10 keV or in the PSPC 0.5–2.4 keV light curves. We will focus thereafter on the average spectral properties only.

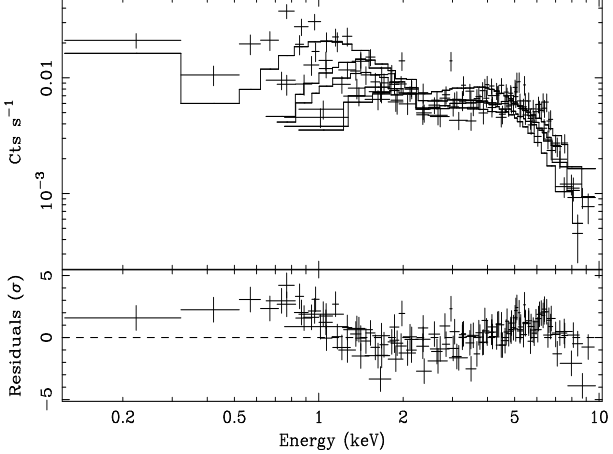


Figure 2. Spectra (*upper panel*) and residuals in units of standard deviations (*lower panel*) when a simple power-law model with photoelectric absorption is applied. Each data point has a signal-to-noise ratio > 5 . Energies in abscissa are in the observer’s frame

4 SPECTRAL ANALYSIS

Fitting separately the same model on the spectra of the ASCA detectors yields consistent results within the statistical uncertainties. Particular care has been adopted in checking the consistency between the PSPC and the ASCA spectra. Several authors have observed a systematic difference in the slopes measured by ROSAT and ASCA in the overlapping energy band, which ranges between 0.2 and 0.4 (cf. Fiore et al. 1994; Iwasawa et al. 1998). Moreover, the source could have varied between the two observations, both in flux and in spectral shape, and the contribution of any diffuse emission from the underlying galaxy could be differently spread underneath the source spot by the instrumental PSF. If we perform a simple power-law fit with photoelectric absorption in the 0.8–2 keV band, the spectral indices turn out to be consistent within the statistical uncertainties ($\Gamma_{\text{ROSAT}} = 1.5 \pm 0.7$, $\Gamma_{\text{ASCA}} = 1.1 \pm 0.3$). Consistent results with those presented in this *Letter* are obtained above 0.5 keV if the ASCA data alone are fitted. At the light of the above considerations, we have fitted the spectra of all detectors simultaneously, allowing relative normalization factors between different detector types as free parameters in all the following fits. Their typical values are always very close to 1 ($N_{\text{GIS}}/N_{\text{SIS}} = 1.02\text{--}1.07$, $N_{\text{PSPC}}/N_{\text{SIS}} = 0.86\text{--}0.92$).

In Figure 2 the spectra and residuals are shown when a simple power-law model with photoelectric absorption by cold matter is applied. The fit is rather bad ($\chi^2_r = 1.59$), mainly due to a prominent soft excess below $\simeq 1.5$ keV and an apparent steepening of the spectrum above $\simeq 7$ keV. A much better χ^2 is obtained if a two-component model is adopted, where the soft excess is parameterized either via a thermal optically thick (blackbody) or thin (`mekal`) plasma or through a broken power-law. In all cases, an emission line is significantly required by the data ($\Delta\chi^2 = 37$), with centroid energy $E_c \simeq 6.35$ keV, consistent with K_α fluorescence from neutral or mildly ionized iron. The 90% upper limit on the Equivalent Width (EW) of a fluorescent He-like (H-like) iron line is 170 eV (140 eV). Table 2 reports

the results and best-fit parameters for all the models described in this section, which yield an acceptable χ^2 . All the phenomenological descriptions are characterized by a very flat hard spectral index ($\Gamma \simeq 0.1$), which is totally inconsistent with that observed in “canonical” spectra of LINERs (Ptak et al. 1998). The observed fluxes in the 0.5–2, 0.5–4.5 and 2–10 keV bands are $\simeq 3.2 \times 10^{-13}$, 1.3 and 3.5×10^{-12} erg cm $^{-2}$ s $^{-1}$, respectively, corresponding to *unabsorbed* luminosities of 3.6×10^{40} , 1.3 and 4.7×10^{41} erg s $^{-1}$, respectively. It is interesting to note that the spectrum *cannot* be modeled with the composition of thermal components alone, regardless of their nature and/or different types of absorption. We have tried three different possible scenarios (albeit not mutually exclusive on physical grounds) to account for the observed flatness: (a) a “partial covering” of a nuclear source; (b) a “pure Compton-reflection” model; (c) a “transmission” model, where the nuclear radiation is seen through a thick screen of absorbing matter. In cases (b) and (c) a soft excess is still required and has been parameterized with either a blackbody, an optically thin plasma with free abundance or a scattering component, *i.e.* a locally unabsorbed power-law with spectral index constrained to be equal to that of the primary power-law. A K_α fluorescent iron emission line is required by all models as well.

The “partial covering” yields a very successful fit ($\chi^2_r = 0.95$). A screen with $N_{\text{H}} \simeq 10^{23}$ cm $^{-2}$, covering $\simeq 80\%$ of the primary source is required. The photon index of the primary continuum is still very flat ($\simeq 1.25$).

The “pure reflection” scenario is also a very good parameterization of the spectrum ($\chi^2_r = 0.90\text{--}0.93$). The intrinsic spectral index turns out to be even steeper than typically observed in Seyferts if the soft excess is modeled through a thermal component ($\Gamma \simeq 2.3$), but perfectly consistent with it if the soft excess is due to scattering of the primary radiation. However, the iron line is rather tiny in this scenario (EW $\simeq 80\text{--}90$ eV).

The “transmission” scenario is again a good model for the data ($\chi^2_r = 0.95\text{--}0.97$). If the soft excess is modeled through scattering or an optically thin plasma, the intrinsic spectral index is again rather flat ($\Gamma \simeq 1.0\text{--}1.4$) and seen through a $N_{\text{H}} \sim 10^{23}$ cm $^{-2}$ screen. The unabsorbed luminosity of the nuclear component is $\simeq 5.6 \times 10^{41}$ erg s $^{-1}$. The iron line EW ranges between 100 and 400 eV.

We have also tried a “mixed transmission+reflection” scenario, assuming that the nuclear primary continuum is not a simple power-law, but is modified by Compton-reflection, probably originating in the putative relativistic Keplerian accretion disk spiraling around the supermassive black hole. In this hypothesis the iron line is expected to be significantly broadened (Matt et al. 1992; Tanaka et al. 1995; Nandra et al. 1997), but the available statistics does not allow us to set any constraint on the line profile. An intrinsic Seyfert-like spectral index is obtained ($\Gamma \simeq 2$), absorbed through a screen of several 10^{22} cm $^{-2}$. However, this is got at the cost of an unplausible high relative normalization between the reflected and primary components ($R \gtrsim 20$). The iron line is again rather weak (EW $\simeq 100$ eV). It is very difficult to imagine a geometry such as to produce this huge amount of reflection when the primary radiation is not completely suppressed in the ASCA bandpass by a Compton-thick absorber, unless the nuclear emission is strongly beamed towards the reflecting matter.

Table 2. Best fit parameters and χ^2 for the combined PSPC/ASCA spectral fits. Explanations of the model abbreviations: *wa* = photoelectric absorption; *pc* = partial covering; *po* = power-law; *bp* = broken power-law *bb* = blackbody; *mk* = MEKAL code (optically thin plasma); *ga* = Gaussian emission line; *px* = Compton-reflection

Power-law + soft excess								
Model	N_{H} (10^{20} cm^{-2})	Γ_{hard}	kT or E_{break} (eV)	Γ_{soft} or Z	E_{c} (keV)	EW (eV)	χ^2/dof	
<i>wa*(po+bb+ga)</i>	$2.3^{+1.6}_{-0.8}$	$0.11^{+0.07}_{-0.08}$	165^{+18}_{-15}		$6.35^{+0.07}_{-0.08}$	220^{+110}_{-70}	313.3/310	
<i>wa*(po+mk+ga)</i>	3 ± 2	$0.11^{+0.08}_{-0.07}$	490 ± 150	$0.07^{+0.59}_{-0.05}$	$6.35^{+0.06}_{-0.07}$	240 ± 80	310.1/309	
<i>wa*(bp+ga)</i>	$4.1^{+1.6}_{-2.0}$	0.15 ± 0.07	$1.42^{+0.16}_{-0.12}$	$1.9^{+0.5}_{-0.3}$	$6.35^{+0.07}_{-0.06}$	240 ± 80	313.4/310	
Partial covering								
Model	N_{H}^1 (10^{20} cm^{-2})	Γ	N_{H}^2 (10^{22} cm^{-2})	C_{f}	E_{c} (keV)	EW (eV)	χ^2/dof	
<i>wa*pc(po+ga)</i>	$2.6^{+0.9}_{-0.8}$	1.21 ± 0.16	$10.3^{+1.8}_{-1.5}$	0.79 ± 0.05	6.36 ± 0.06	230^{+80}_{-90}	296.9/310	
Pure reflection+soft excess								
Model	N_{H} (10^{20} cm^{-2})	Γ	kT (eV)	Z or $f_{\text{s}} \times (2\pi/\Omega)$	E_{c} (keV)	EW (eV)	χ^2/dof	
<i>wa*(px+po+ga)</i>	$5.0^{+0.9}_{-0.8}$	$2.16^{+0.16}_{-0.14}$		$0.0033^{+0.0011}_{-0.0016}$	6.4^{\dagger}	80^{+70}_{-30}	290.8/312	
<i>wa*(px+bb+ga)</i>	$3.5^{+1.3}_{-0.9}$	2.43 ± 0.09	190 ± 30		6.4^{\dagger}	90 ± 70	283.0/311	
<i>wa*(px+mk+ga)</i>	$4.3^{+1.3}_{-1.0}$	$2.42^{+0.10}_{-0.09}$	620^{+170}_{-150}	$0.05^{+0.20}_{-0.04}$	6.4^{\dagger}	90^{+100}_{-70}	278.0/309	
Transmission + soft excess								
Model	N_{H}^1 (10^{20} cm^{-2})	Γ	N_{H}^2 (10^{22} cm^{-2})	kT	f_{s} or Z (keV)	E_{c}	EW (keV)	χ^2/dof (eV)
<i>wa*[wa*(po+ga)+po]</i>	$2.6^{+0.9}_{-0.7}$	1.22 ± 0.16	12 ± 2		$0.26^{+0.15}_{-0.09}$	6.36 ± 0.06	300 ± 110	297.0/310
<i>wa*[wa*(po+ga)+bb]</i>	< 1.8	$0.49^{+0.20}_{-0.19}$	$1.7^{+1.1}_{-0.8}$	260 ± 50		$6.36^{+0.06}_{-0.07}$	260 ± 90	299.3/309
<i>wa*[wa*(po+ga)+mk]</i>	$2.5^{+0.8}_{-0.6}$	$1.0^{+0.5}_{-0.4}$	9^{+6}_{-3}	> 9	1^{\dagger}	$6.35^{+0.07}_{-0.06}$	220 ± 110	296.0/309
Mixed transmission + reflection								
Model	N_{H}^1 (10^{20} cm^{-2})	Γ	N_{H}^2 (10^{22} cm^{-2})	f_{s}	R	E_{c} (keV)	EW (eV)	χ^2/dof
<i>wa*[wa*(po+ga+px)+po]</i>	$5.5^{+1.7}_{-1.6}$	$2.1^{+0.2}_{-0.4}$	$3.0^{+1.9}_{-1.8}$	$0.5^{+0.2}_{-0.2}$	80^{+0}_{-60}	$6.38^{+0.08}_{-0.14}$	100^{+90}_{-80}	280.6/309

† fixed

5 DISCUSSION AND CONCLUSIONS

The X-ray spectrum of the LINER NGC 1052 is exceptionally flat. The observed 2–10 keV photon index is $\Gamma \simeq 0.1$. The 2–10 keV luminosity in the same energy range ($\sim 5 \times 10^{41} \text{ erg s}^{-1}$) is more than one order of magnitude higher than the expected contribution from unresolved Low Mass X-Ray Binaries within the galaxy (Canizares et al 1987; Matsushita et al. 1994). Models to explain such a spectrum fall in two main classes: those which require a highly absorbed ($N_{\text{H}} \simeq 10^{23} \text{ cm}^{-2}$) transmitted power-law; (“partial covering” and “transmission” scenarios); and those where the 2–10 keV flux is dominated by Compton-reflection (“pure reflection” scenario).

In the former cases, the spectral index is still rather flat ($\Gamma \simeq 1.0$ – 1.4). Such values are distant from the average observed in Seyferts (Nandra et al. 1997), although not uncommon among type-2 objects (Smith & Done 1996; Turner et al. 1997). Alternatively, such a flat index emerges naturally if accretion occurs via an advection-dominated flow (ADAF, Narayan & Yi 1995). ADAF has been recently invoked to explain the emission from low-luminosity AGN, thanks to the very low radiative conversion efficiency that characterizes it. It has been rather successful in modeling the Spectral Energy Distributions of some low-luminosity AGN (see *e.g.*: Narayan et al. 1998). It has been recently pointed out that the canonical model significantly overestimates the radio and sub-millimeter flux in a number of ellip-

tical galaxies, hence suggesting the existence of mechanisms to suppress the emission from the central region at these wavelengths (Di Matteo et al. 1998). In the basic ADAF scenario the X/ γ -ray emission should be dominated by thermal bremsstrahlung due to the very hot electron distribution in the disk, with typical kT ~ 100 keV. In low-resolution, band-limited detectors such a spectrum might be well approximated by a simple power-law with $\Gamma \simeq 1.4$. Further observations covering the energy band up to a few hundreds keV might be very valuable in assessing the viability of such a scenario, and are nowadays possible thanks to the unprecedented sensitivity of the Phoswitch Detector System on board BeppoSAX.

If the transmission scenario is true in NGC 1052 (either in the Sakura-Sunayev or in the ADAF flavor), two more ingredients are needed: *i*) a screen of cold absorbing matter of $N_{\text{H}} \simeq 10^{23} \text{ cm}^{-2}$, which could be provided by the “torus” envisaged by the unification scenario or (in the ADAF case) by the cold outermost regions of a geometrically bloated disk. The observed iron line is consistent with being produced by the same absorbing screen, even if a contribution to the iron line comes from a relativistic, X-ray illuminated disk close to the nuclear black hole (note that an ADAF should not intrinsically produce any fluorescent line); *ii*) a soft component, either as partial covering, or as a thermal emission peaking at several keV or as an energy-independent $\simeq 25\%$ scattering of the primary radiation. The discovery of broad optical polarized lines advocates for scattering indeed to occur in

NGC 1052. However, there is evidence for an extended soft X-ray component from the HRI data, which is likely to be associated with the diffuse emission of the galaxy. The limited spectral resolution of the HRI does not allow a self-consistent determination of the luminosity of such a component. If one assumes that it is thermal in origin with a temperature of 0.5 keV (comparable to those typically observed in elliptical galaxies; cf. Fabbiano 1989), the implied 0.1–2 keV luminosity is $\sim 3 \times 10^{40}$ erg s⁻¹. From the observed correlation between the blue and the X-ray luminosities in ellipticals (David et al. 1992), one may expect a contribution to the 0.5–4.5 keV luminosity from the diffuse galaxy emission of the same amount (David et al. 1992). Of course different components could be simultaneously present in the soft X-ray band, thus confusing the interpretation of the data. A detailed modeling of the soft excess in NGC 1052 requires experiments with much higher spatial resolution and/or effective area.

Alternatively, a Compton reflection-dominated spectrum from a “canonical” Seyfert-like primary spectrum provides an equally good parameterization of the data. However, in this case the iron line is very faint, the EW being one order of magnitude lower than observed in Compton-thick Seyfert 2s so far (Iwasawa et al. 1997; Matt et al. 1996b; Maiolino et al. 1998) and expected on theoretical grounds (Ghisellini et al. 1994; Matt et al. 1996a). In principle, a strong iron under abundance could resolve the discrepancy, although it is not clear why this should be the case in the nucleus of an elliptical galaxy. Moreover, there is currently no observational evidence for iron under-abundance in AGN central regions. A more appealing solution may be that the surface of the inner disk is ionized of such an amount that the bulk of the line flux is suppressed via resonant trapping (Matt et al. 1993). We would therefore be observing only a minority of the line flux, emerging from the outermost and cold parts of the disk. However, it is difficult to imagine a geometry where the inner regions of the disk are visible, while the primary nuclear emission is totally suppressed.

While a wide literature exists on the optical spectra of LINERs, the X-ray spectrum of only a few objects has been studied in detail. In this *Letter* we have presented evidence that an obscured ($N_{\text{H}} \sim 10^{23}$ cm⁻²) AGN, possibly accreting via an ADAF, is the ultimate source powering NGC 1052. Undoubtedly, future X-ray observations will contribute to further enlighten the connection between LINER phenomenon and nuclear activity, and the nature of the accretion processes occurring in LINERs.

ACKNOWLEDGMENTS

The authors acknowledge valuable discussions with F. Fiore and G. Matt, which greatly improved the quality of the paper. MG acknowledges an ESA research fellowship. This research has made use of the NASA/IPAC Extragalactic Database, which is operated by the Jet Propulsion Laboratory, Caltech, under contract with NASA, and of data obtained through the HEASARC on-line service, provided by NASA/GSFC.

REFERENCES

- Antonucci R. R. J., 1993, *ARAA*, 31, 473
 Barth A.J., 1998, Ph.D. thesis, Univ. California Berkeley
 Becklin E.E., Tokunaga A.T., Wynn-Williams C.G., 1982, *ApJ*, 263, 624
 Canizares C.R., Fabbiano G., Trinchieri G., 1987, *ApJ*, 312, 503
 Claussen M.J., Diamond P.J., Braatz J.A., Wilson A.S., Henkel C., 1998, *ApJ*, 500, 129
 David L.P., Jones C., Forman W., 1992, *ApJ*, 388, 82
 De Vaucouleurs, 1991, “Third reference Catalog of Bright Galaxies”, *Science*, n.254, 5038, 1667
 Di Matteo T., Fabian A.C., Rees M.J., Carilli C.L., Ivison R.J., 1998, *MNRAS*, in press (astroph/9807245)
 Disney M.J., Wall J.V., 1977, *MNRAS*, 179, 235
 Fabbiano G., 1989, *ARA&A*, 27, 87
 Fabbiano G., Juda J.Z., 1997, *ApJ*, 476, 666
 Fiore F., Elvis M., McDowell J.C., Siemiginowska A., Wilkes B.J., 1994, *ApJ*, 431, 515
 Fosbury R.A.E., Mebold U., Goss W.M., Dopita M.A., 1978, *MNRAS*, 183, 549
 Fosbury R.A.E., Sijnders M.A.J., Bokseberg A., Penston M.V., 1981, *MNRAS*, 197, 235
 Garcia A.M., 1993, *A&ASS*, 1993, 100, 47
 Ghisellini G., Haardt F., Matt G., 1994, *MNRAS*, 267, 743
 Heckman T.M., 1980, *A&A*, 88, 365
 Ho L.C., 1998, in “Evidence for Black Holes in the Universe”, Chakrabarti S.K. ed. (Dordrecht:Kluwer), in press
 Ho L.C., 1999, *Adv. Sp. Res.*, in press (astroph/9807273)
 Ho L.C., Filippenko A.V., Sargent W.L.W., Peng C.Y., 1997, *ApJS*, 112, 391
 Huchra J.P., Geller M.J., 1982, *ApJ*, 257, 423
 Iwasawa K., Comastri A., 1998, *MNRAS*, 297, 1291
 Iwasawa K., Fabian A.C., Brandt W.N., 1998, *MNRAS*, 293, 251
 Iwasawa K., Fabian A. C., Matt G., 1997, *MNRAS*, 289, 443
 Koraktar A.P., Deustua S., Heckman T.M., Filippenko A.V., Ho L.C., Rao M., 1995, *ApJ*, 440, 132
 Makishima K., et al., 1996, *PASJ*, 48, 17
 Matsushita K., et al., 1994, *ApJL*, 436, L41
 Matt G., Brandt W.N., Fabian A.C., 1996a, *MNRAS*, 280, 823
 Matt G., Fabian A.C., Ross R.R., 1993, *MNRAS*, 261, 346
 Matt G., Fiore F., Perola G. C., Piro L., Fink H. H., Grandi P., Matsuoka M., Oliva E., Salvati M., 1996b, *MNRAS*, 281, L69
 Matt G., Perola G.C., Piro L., Stella L., 1992, *A&A*, 257, 63 (erratum 263,453)
 Matt G., et al., 1997, *A&A*, 325, L13
 Maiolino R., Salvati M., Bassani L., Dadina M., Della Ceca R., Matt G., Risaliti G., Zamorani G., 1998, *A&A*, 338, 781
 Nandra K., George I.M., Mushotzky R.F., Turner T.J., Yaqoob Y., 1997, *ApJ* 477, 602
 Nandra K., Pounds K.A., 1994, *MNRAS*, 268, 405
 Narayan R., Mahadevan R., Grindlay J.E., Popham R.G., Gammie C., 1998, *ApJ*, 492, 554
 Narayan R., Yi I., 1995, *ApJ*, 452, 710
 Ptak A., Serlemitsos P., Yaqoob T., Mushotzky R.F., 1998, *ApJ*, in press (astroph/9808159)
 Sadler P.M., 1987, *S&T*, 74, 452
 Smith D.A., Done C., 1996, *MNRAS*, 180, 355
 Tanaka Y., Inoue H., Holt S.S., 1994, *PASJ*, 46, L37
 Tanaka Y., et al., 1995, *Nature*, 365, 659
 Terashima Y., Kunieda H., Misaki K., Mushotzky R.F., Ptak A.F., Reichert G.A., 1998, *ApJ*, 503, 212
 Turner T.J., George I.M., Nandra K., Mushotzky R.F., 1997, *ApJS*, 113, 23
 Worrall D.M., Birkinshaw M., 1994, *ApJ*, 427, 134